GRC Transactions, Vol. 42, 2018

Experimental Study of Thermal-Crack Characteristics on Hot Dry Rock Impacted by Liquid Nitrogen Jet

Shikun Zhang, Zhongwei Huang*, Hongyuan Zhang, Xiaoguang Wu, Chengcheng Zhang, Chao Xiong

State Key Laboratory of Petroleum Resources and Prospecting, China University of Petroleum-Beijing, Beijing 102249, China

Keywords

Thermal cracks; HDR fracturing; Liquid nitrogen jet; Experimental test; Fractal method;

ABSTRACT

Liquid nitrogen jet fracturing is a novel stimulation technology, which is expect to be suitable for hot dry rock (HDR) reservoirs. Due to the large temperature difference between hot rock and cryogenic fluid, a great number of thermal cracks would be created during fracturing process, which is conductive to improve the penetration capacity of formation. In this study, a set of experiments are conducted to investigate the characteristics of thermal cracks. In these experiments, the granite specimens with temperatures ranging from 200℃ to 300℃ are impacted by the low-pressure liquid nitrogen jet. The complexity and connectivity of cracks are quantitatively analyzed by a fractal method. The permeability and ultrasonic velocity of granite specimens are tested in order to evaluate the damage conditions caused by thermal stress. The experimental results show that the cracks induced by thermal stress mainly concentrate in the region near impingement surface, due to the large temperature gradient there. With the rise of initial rock temperature, the number of thermal cracks increases, and a more complex crack-network is formed in each specimen. Transient pulse evaluation and ultrasonic velocity measurements indicate that the impact of liquid nitrogen jet can improve the permeability and cause the damage of hot rock noticeably. This study demonstrates the important effect of thermal stress on crack generation during liquid nitrogen jet fracturing for HDR reservoirs, and the results shed light on the exploitation of HDR energy.

1. Introduction

Hot dry rock (HDR), as an abundant, clear and wide-spread energy, has been considered as one of the most potential renewable resources in the future (Caulk et al., 2016; Shi et al., 2018). It was reported that the total HDR heats stored within subsurface of 3–10 km depths in the United States and China can reach about 1.4×10^{25} J and 2.52×10^{25} J respectively (Panel, 2006; Wang et al.). The Enhanced Geothermal Systems (EGS) is an efficient means to extract the heat from deep formations, by circulating the working fluid between injection wells and production wells (Grant, 2015). However, the permeability of HDR reservoirs is normally pretty low, making it difficult for fluid to flow in these formations. Therefore, stimulation treatments need to be performed to commercially exploit the HDR resources (Zimmermann and Reinicke, 2010).

Some stimulation methods have been developed to improve the HDR permeability, such as, hydraulic fracturing (Legarth et al., 2005), thermally induced fracturing (Charlez et al., 1996) and chemical stimulation (Nami et al., 2008). At present, hydraulic fracturing is considered as the most effective means, which has been widely applied in oil and gas industry (Gale et al., 2007; Sun et al., 2017). However, the single large fracture is normally generated during hydraulic fracturing, which is not expected in EGS project. In order to increase heat transfer area in formation, the multiple fractures or reticular fractures are set as a target in HDR fracturing process (Zhou et al., 2018). The hydraulic jet fracturing technology by integrating abrasive jet perforating, hydraulic fracturing and hydrodynamic sealing, can achieve the multi-stage fracturing with a lower initiation pressure (Li et al., 2010; Sheng et al., 2013). Nevertheless, this method consumes a large amount of water, and still cannot create the suitable fracture structures in formation for HDR exploitation.

The novel waterless fracturing technology, liquid nitrogen fracturing has been successfully used in some oil and gas wells (Grundmann et al., 1998; McDaniel et al., 1997). Field applications indicate that the performance of wells was improved noticeably after the stimulation of liquid nitrogen, and little damage was caused to casing integrity. Researchers also carried out a series of laboratory experiments and numerical simulations to investigate the feasibility of liquid nitrogen as a fracturing fluid. The experiment by Cha et al. (Cha et al., 2014) shows that huge thermal stresses are generated in rock surrounding the wellbore during cryogenic fluid fracturing. Theses stresses are mainly in the form of tensile stress, which would promote the generation and extension of cracks in formation. Zhang et al. (Zhang et al., 2018b) built a 3D model to analyze the heat transfer and thermal-stress distribution in bottom-hole rock during liquid nitrogen fracturing process. The simulation results support the view of Cha et al. (Cha et al., 2014), and show that the tensile stress induced by rapid cooling far exceeds the tensile strength of common rocks. Cai et al. (Cai et al., 2015) evaluated the thermal effect of liquid nitrogen on coal damage by laboratory experiment. Their study indicates that coal permeability increases by 48.89%-93.55% because of liquid nitrogen super-cooling. The research by Perkins and Gonzalez (Perkins and Gonzalez, 1985) shows that the secondary cracks generated by thermal effect are perpendicular to the main cracks, which are beneficial to form a complex fracture structure in formation. Considering the unique low-temperature characteristic, Zhang et al. (Zhang et al., 2018a) proposed to use liquid nitrogen to fracture the HDR reservoirs. In fracturing operation, the liquid nitrogen is injected into formation with high pressure and large displacement firstly, to create a single or several large cracks. Then, the reservoir is impacted by the liquid nitrogen with a low flow rate for a long time. The cryogenic fluid would enter into the existing cracks and create new thermal cracks in formation. The expected fractures pattern in liquid nitrogen fracturing for HDR reservoir is shown as **Fig. 1**.

However, liquid nitrogen lacks of adequate viscosity to carry proppant flowing in reservoir (Rudenko and Schubnikow, 1968). Raising flow rate may improve the proppant carrying ability of working fluid (Gupta and Bobier, 1998), whereas this method would put a huge burden on pumps and pipelines as well. To adapt the low viscosity of liquid nitrogen, ultra-light weight proppants can be used in fracturing operation (Kendrick et al.). In addition, some researches even show that fracturing with cryogenic fluid could rely on self-propping means to keep artificial fracture open (McDaniel et al., 1997). Nevertheless, whether the cracks generated in cryogenic fluid fracturing can meet the demands of fluid flow in reservoir, need to be further investigated.

Researchers have employed diverse methods to evaluate the properties change of fractured rock. Kim and Kemeny (Kim and Kemeny, 2009) investigated the influence of thermal impact on the rock mechanical properties by supersonic wave velocity and tensile strength tests. Cai et al. (Cai et al., 2014) used the methods of scanning electron microscope (SEM) and nuclear magnetic resonance to evaluate the rock damage cooled by liquid nitrogen. Based on the experiments, the crack-structure changes and the micro-fissure distribution can be characterized. The pressure-decay tests was employed by Cha et al. (Cha et al., 2018) to measure the permeability change of rock specimen treated by liquid nitrogen. For fracturing cracks, the fractal method is one of the most useful means to quantitatively describe the complexity and connectivity. Researches (Liu et al., 2016; Roy et al., 2007) show that the permeability as well as the porosity of fractured rock has a good correlation with the fractal dimension.

In the process of HDR fracturing with liquid nitrogen, the thermal cracks would play a vital role to improve the formation permeability and connectivity. This study carried out a set of experiments to investigate the cracks induced by thermal stress. In experiment, the hot granite rocks were impacted by the low-pressure liquid nitrogen jet. The distribution of thermal cracks was analyzed by a fractal method. The permeability and ultrasound velocity were measured to evaluate the effect of liquid nitrogen jet on hot rock. The microscopic features of thermal cracks were presented by SEM observation.

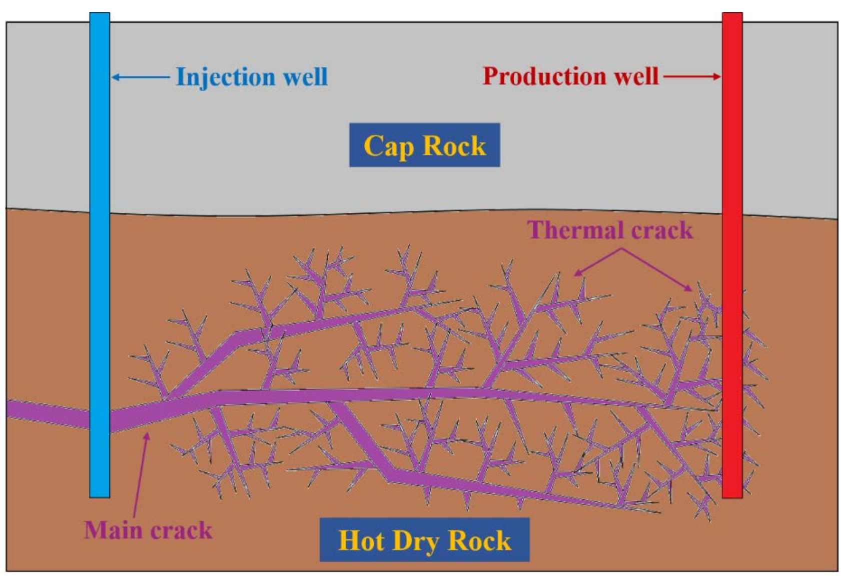

Figure 1: Schematic diagram of fracture mode in liquid nitrogen fracturing

2. Experiment Design

2.1 Granite Specimens

In this experiment, the granite rock is selected as the impacted specimen, which is common for HDR reservoirs. Our previous research (Zhang et al., 2018a) shows that the specimen size has a vital influence on the generation of thermal cracks in rock when impacted by liquid nitrogen jet. Since the limitation of laboratory conditions, the specimen boundaries cannot be effectively fixed in experiment, which affects the thermal-stress distribution noticeably. The previous experiments indicate that there are few thermal cracks generated on specimen (150×150×100 mm) with temperature below 300 ℃. Increasing the size of specimen can reduce the effect of free-boundary. In this study, the rectangular specimen with size of 200×200×100 mm is adopted in impingement experiment. No obvious natural fractures exist on the surfaces of granite specimen, and other physical properties are shown in **Table 1**

Table 1 Physical properties of granite specimen

Rock parameters	Values
Density	2640 kg/m^3
Young's modulus	26.47 GPa
Poisson ratio	0.1050
Uniaxial tensile strength	4.210 MPa
Uniaxial compressive strength	84.47 MPa

2.2 Experimental Equipment

The purpose of this study is to investigate the characteristics of thermal cracks. Therefore, the low-pressure liquid nitrogen jet is employed in impingement experiment, in which the effect of liquid pressure on hot rock is small. The cracks in specimens are mainly created by the impact of thermal stresses.

The schematic diagram of experimental setup used to form low-pressure liquid nitrogen jet is shown as **Fig. 2**. It contains three parts, the gas cylinder, self-pressurization storage tank and fixed bracket. The liquid nitrogen is provided by the self-pressurization tank, which can pressurize the fluid up to 3.45 MPa by vaporizer. However, the pressure in self-pressurization tank is not stable because of the low evaporation rate in heating coil. Therefore, the high-pressure gas cylinder is adopted to maintain pressure stability in tank. The fixed bracket is used to fix the nozzle and adjust the injection standoff distance in this experiment. Due to the low acting force of liquid nitrogen jet and heavy weight of specimen, the rock need not to be fixed during experiment.

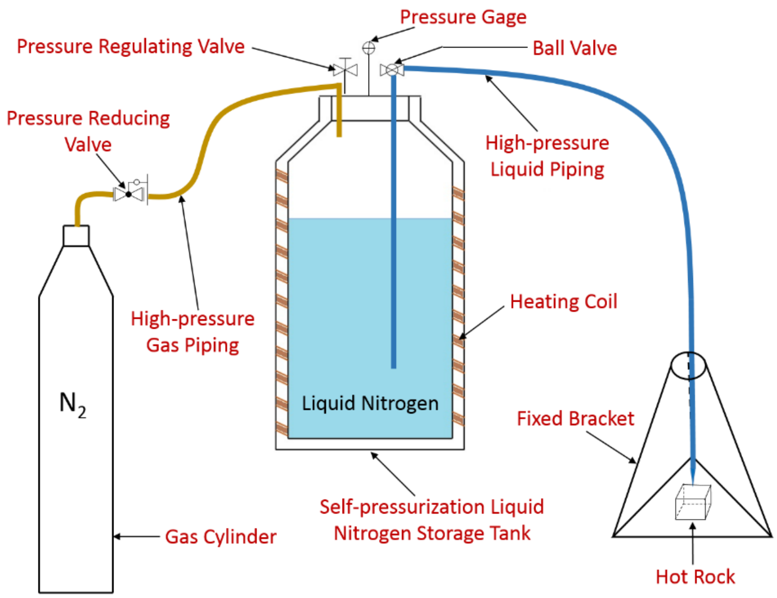

Figure 2: Schematic diagram of experimental setup

The rock permeability is measured by the high-pressure gas permeameter after impingement experiment. The nitrogen gas is adopted as the working fluid of permeability tester due to the low permeability of granite. The permeability tester and ultrasonic tester used in experiments are shown in **Fig. 3** and **Fig. 4** respectively.

Figure 3: High-pressure gas permeameter

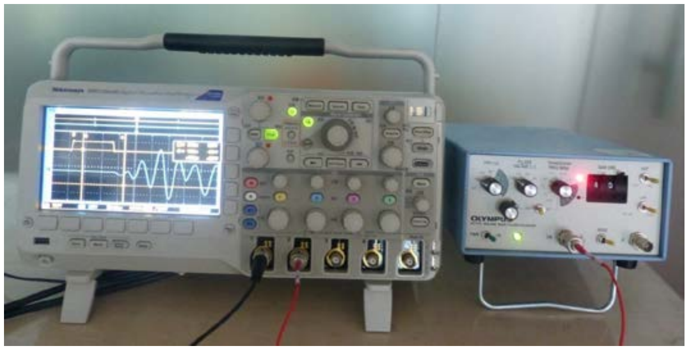

Figure 4: Olympus ultrasonic tester

2.3 Experiment Schedule

In order to investigate the influence of rock temperature on thermal-crack generation, the specimens were heated to five different temperatures, varying from 220 ℃ to 300 ℃. For each rock temperature, three repeated experiments were conducted. The specimens were heated by the muffle furnace with heating rate being 10 ℃ per hour. The total heating time of each specimen was 48 hours to ensure the temperature homogeneity. After being taken out from furnace, the hot specimens were insulated by the asbestos immediately, and then impacted by the low-pressure liquid nitrogen. The specific injection parameters are shown in **Table 2**.

Table 2 Injection parameters

Injection parameters	Values
Liquid temperature	-196 ℃
Liquid pressure	2.5 MPa
Standoff distance	1 mm
Duration time	2 min

Since the large size of the specimen, it needs to be further processed before the permeability and ultrasonic tests. However, the thermal cracks distribute randomly on the impingement surface. Therefore, two standard cores ($\phi 25 \times 50$) were drilled from every large specimens to better describe the thermal-crack characteristics. The coring positions are shown in **Fig. 5**. Additionally, three standard cores from the specimen which was not treated by liquid nitrogen jet were prepared as comparison samples.

Before the permeability test, the standard cores were put in the drying oven with constant temperature of 60 ℃ for 8 hours. The inlet pressure of permeability tester was 0.4 MPa, and the ambient pressure was 0.2 MPa during the test process. Half hour later after the pressure remained unchanged, the gas flow rate was measured. Based on the Darcy law, the rock permeability can be calculated by using the gas flow rate and the pressure drop between inlet and outlet. In the ultrasound test, the P-wave velocity was measured. The damage of impacted rock can be evaluated by comparing the P-wave velocities of specimen before and after liquid nitrogen jet impact.

Figure 5: Coring positions of standard cores in granite specimen

3. Experimental Results and Discussion

3.1 Thermal-Crack Distribution

Our previous work (Zhang et al., 2017) has shown that huge tensile stresses would be formed in the region near impingement surface. These stresses far exceed the rock tensile strength, and can have an important effect on rock fracturing. In this study, the rock boundaries did not have effective constrains, causing the thermal stresses smaller than that in simulation. However, the tensile strength of granite specimen using for experiment is just 4.210 MPa. Therefore, the thermal induced stresses can create numerous thermal cracks in specimen.

Fig. 6 shows the thermal-crack distribution in granite specimen with different initial temperatures. Since the thermal cracks would close when specimens drop to room temperature, the black lines were used to represent the cracks in figure. It can be noticed that only several short thermal cracks are generated in rock with a relatively low temperature (220℃). As the rise of initial rock temperature, the number of thermal cracks increases, and more cracks get connected together. Some large cracks have even cut through the impingement surface when initial rock temperature exceeds 280℃. It also can be found that most thermal cracks initiate from the margin region, and extend to the center of rock specimen. That may result from the low constrain in margin region. Additionally, the crack is more likely to extend along the cementing edge of different mineral grains in granite specimen.

3.2 Fractal Analysis

In order to quantitatively evaluate the characteristics of thermal cracks, the fractal method is employed. In this method, the fractal dimension (*D*) is closely related to the connectivity and compactness of crack network (Cai et al., 2017; Xu et al., 2016), which is calculated by an improved box-counting technique (Roy et al., 2007). In calculation process, the mapped fracture system is superimposed by square box with size of *r*. The relationship between fractal dimension and the number of the occupied boxes covering fracture *N(r)* is shown as **Eq. (1)**.

$$N(r) \propto r^{-D} \tag{1}$$

The fractal dimension can be obtained by linearly fitting the data points in *log-log* space (*N(r)* versus *r*). According to improved box-counting algorithm, the cutoff box size r_{cmin} is determined by the standard deviation of slope *s*, written as **Eq. (2)**.

$$s = \sqrt{\frac{\sum_{i=1}^{m}(y_i - y_{ai})^2}{(M-2)\sum_{i=1}^{m} x_i^2}} \tag{2}$$

Where, y_i and y_{ai} are observed *lnN(r)* and predicted *lnN(r)* respectively; $x_i = ln(r)$; M is the observation number. The cutoff box size is equal to the value of minimum box size, as the variable *ds/dr* approaches to zero.

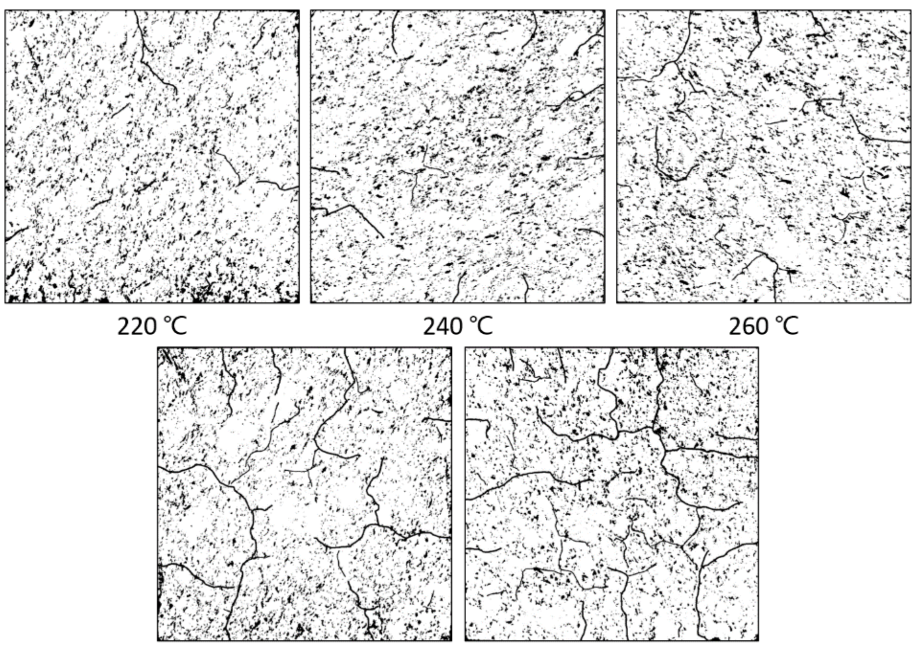

Figure 6: Thermal cracks distribution in specimens with different initial temperatures

The calculating result indicates that the thermal cracks have a good fractal characteristic, with the maximum R^2 up to 0.996. **Fig. 7** illustrates the average fractal dimensions and standard errors of crack networks in different rock temperatures. As the analysis in section **3.1**, raising initial rock temperature can significantly increase the number and the complexity of the thermal cracks. Consequently, the fractal dimension of crack network rises. However, due to the random distribution of thermal cracks, there exist some differences of fractal dimensions between repeated experiments with the same rock temperature. The fractal dimensions in this study values from 1.220 to 1.315, which are in the range of 1.22-1.38 given by Zhang and Sanderson (Zhang and Sanderson, 1994). According to the study of Wang et al. (Wang et al., 2015), the permeability as well as porosity of fractured rock shows a power-law relationship with the fractal dimension. Thus, the temperature of reservoirs can have a vital influence on the complexity of thermal cracks during liquid nitrogen fracturing.

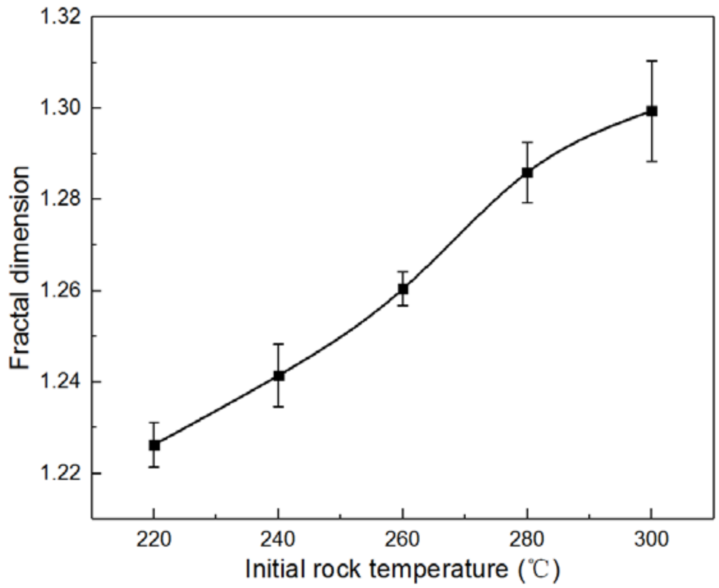

Figure 7: The fractal dimension of thermal cracks

3.3 Permeability Variation

The cracks induced by thermal stress can have an important effect on rock permeability. **Fig. 8** shows the thermal-crack distribution on standard-core surface. The cores were drilled from the center of large specimens. Among them, the specimen in **Fig. 8 (a)** is the control sample, which does not be heated and impacted by liquid nitrogen jet. It is noticed that there are few obvious cracks on the untreated specimen. For the specimen with initial temperature being 220 ℃, shown in **Fig. 8 (b)**, several cracks distribute on the impingement surface. However, the cracks are small, and could not connect with each other. When the rock temperature rises to 300 ℃, some large cracks are generated on specimen surface, shown as **Fig. 8 (c)**. These large cracks run through the specimen, which may improve the permeability significantly.

Fig. 9 illustrates the distribution of thermal cracks in side surfaces of the same specimens in **Fig. 8**. It can be found that the small cracks on specimen with temperature of 220 ℃ do not extend downward. Only surface region is broken by thermal stress. For the rock with high temperature (300 ℃), the huge thermal stress promotes the extension of crack along impingement direction. However, the extended distance of thermal cracks (presented by red line in figure) is finite, at about 10 mm. Under the conditions of fracturing operation, the downhole pressure can reach tens of MPa. The high pressure would make the cryogenic fluid enter into the thermal cracks and induce secondary cracks. After this repeated process, the cryogenic working fluid may spread a long distance in formtion. Nevertheless, the experiments in this study are carried out at atmospheric pressure due to the limitation of experimental equipments. Therefore, the affected region of thermal stress in laboratory experiment may much smaller than that in field application.

Figure 8: Thermal-crack distribution on standard-core surfaces

Figure 9: Thermal-crack distribution on side surfaces

Fig. 10 shows the permeability of specimens with different temperatures. The average permeability of untreated granite rock in this study is about 0.019 mD. With the rise of initial temperature, the rock permeability after impacted by liquid nitrogen jet increases significantly. The average permeability of specimen in different positions with temperature of 300 ℃ is 0.045 mD and 0.063 mD, increasing135.1% and 228.6% respectively, compared with the value of untreated specimen. As the analysis above, the permeability in the region near impingement surface would much larger. It also can be noticed that when the rock with high temperature

(300 ℃), the permeability in margin region (Position 2) is remarkably higher than that in center region (Position 1). That might be because the large cracks in center region is more likely to close when specimen cools to room temperature. However, due to the heterogeneity of granite specimen and the random distribution of thermal cracks, the test data exists some errors, and the maximum standard error can reach 0.0066 mD.

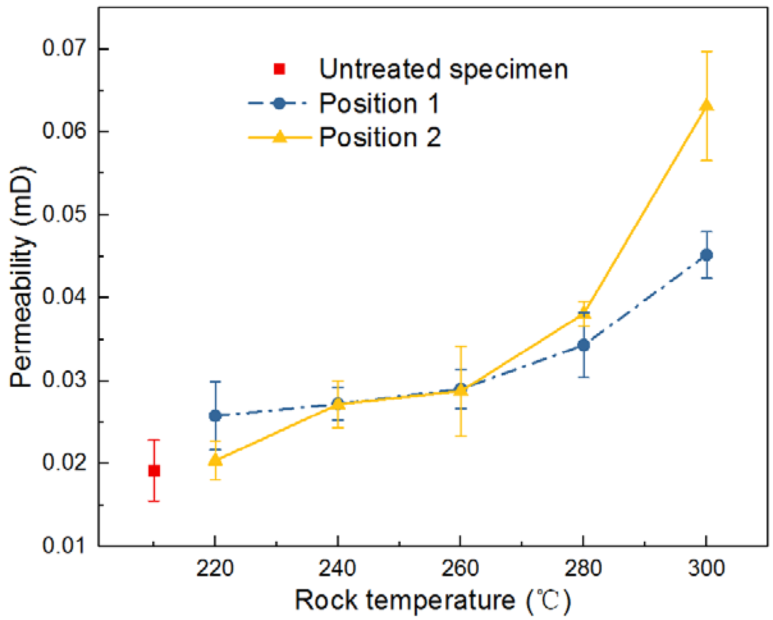

Figure 10: Permeability of specimens with different temperatures

3.4 Damage of Fractured Rock

The P-wave velocity in ultrasound test is normally used to evaluate the rock damage condition. The crack density and distribution are the main factors affected the velocity of P-wave throughout rock specimen. The more the cracks are, the lower the P-wave velocity is. **Fig. 11** shows the P-wave velocities in specimen with different temperatures. It can be noticed that the P-wave has a high velocity in untreated specimen, about 4630 m/s. As rock temperature goes up, the acoustic wave velocity gradually decreases, at a mere 3159 m/s in Position 1 and 3099 m/s in Position 2 when rock temperature is 300 ℃.

A damage factor has been defined in reserch († et al., 1988) which is related to the P-wave velocity, shown as **Eq. 3**.

$$D = 1 - \left(\frac{V_p}{V_{pf}}\right)^2 \tag{3}$$

Where, D represents the damage factor; V_p and V_{pf} are the P-wave velocities in impacted rock and in untreated rock respectively.

Fig. 12 shows the damage factors of impacted specimens with different temperatures. The damage factors see the similar trends in Position 1 and Position 2, which increase with the rise of rock temperature. The maximum damage factor can reach 0.55 when rock temperature is 300 ℃. The result indicates that the hot rocks have been severely damaged by the impact of liquid nitrogen jet. Research (Enayatpour et al., 2013) has indicated that when the rock is rapidly cooled by liquid nitrogen, the tensile stress would induce between rock particles with similar properties, and the shear stress would induce as the particles are much different with each other. The granite specimens using in this study has strong heterogeneity. Therefore, both tensile and shear stress may create in specimen during experiment. These thermal stresses promote the generation of new cracks and the extension of pre-existing cracks. That is probably the reason for the increase of rock-damage factor after the impact of liquid nitrogen jet.

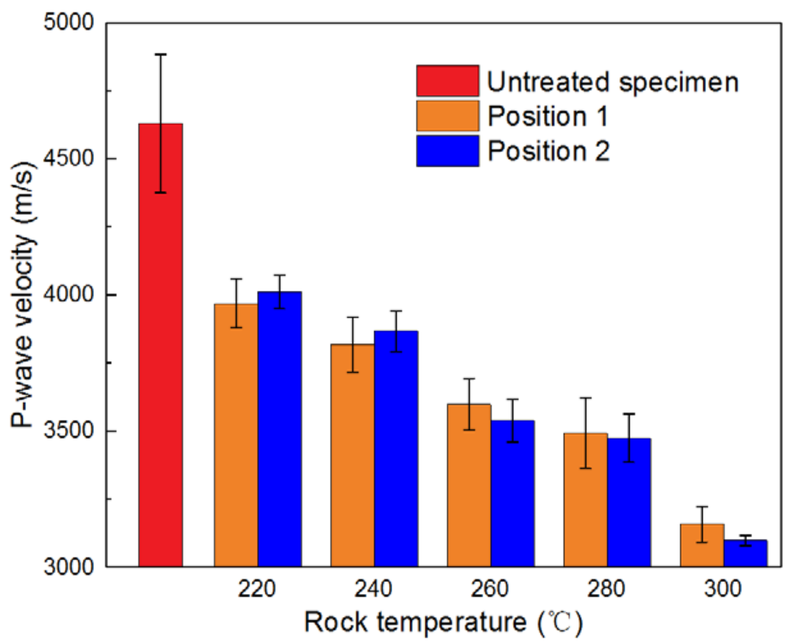

Figure 11: P-wave velocities in specimens with different temperatures

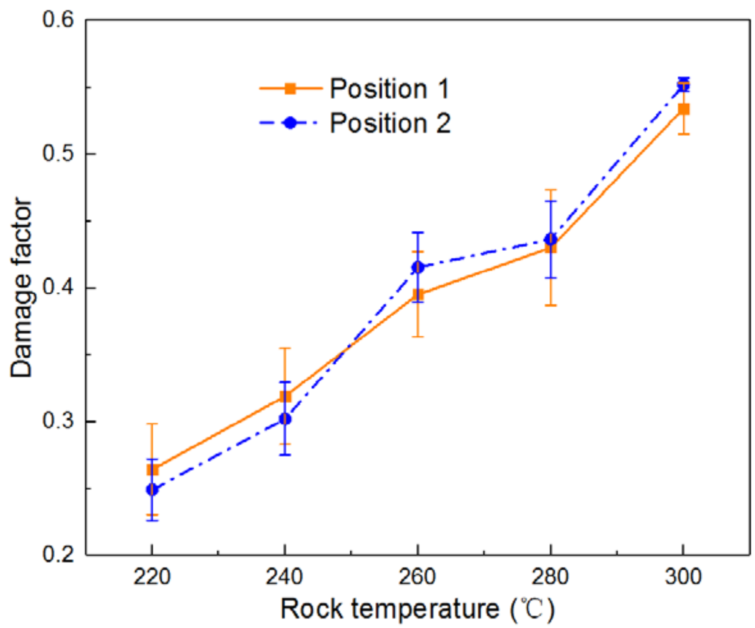

Figure 12: Damage factors of specimens with different temperatures

4. Conclusion

In this paper, the experiment, in which the hot rocks are impacted by low-pressure liquid nitrogen jet, is conducted. A fractal method is employed to analyze the connectivity of thermal cracks. Additionally, the permeability test and ultrasound velocity test are carried out to quantitatively characterize the damage of treated specimens. Based on the results of this study, the following conclusions are drawn:

(1) Numerous thermal cracks are generated in granite specimens when impacted by liquid nitrogen jet. As rock temperature raising, the number and the size of thermal cracks increase. Some large cracks even run through the impacted specimen.

(2) The fractal analysis indicates that the cracks generated by thermal stress have a good fractal feature. The fractal dimension increases with rock temperature rising, which means the connectivity of the impacted specimen is improved.

(3) The thermal cracks only distribute on the impingement surface of impacted rock with relatively low temperature (200 ℃). When the rock temperature raises to 300 ℃, the thermal cracks can extend downward for a certain distance. However, the cracks significantly enhance the specimen permeability, and the maximum increase can be up to 228.6% in experiments.

(4) The ultrasound test shows the P-wave velocity decreases with the rise of rock temperature. The damage factor can reach 0.55 when the rock temperature is 300 ℃. That demonstrates that the hot rock has been severely damaged by the impact of liquid nitrogen jet.

REFERENCES

†, T.K., ‡, Y.I., §, T.K., 1988. Deformation and fracturing behaviour of discontinuous rock mass and damage mechanics theory. International Journal for Numerical & Analytical Methods in Geomechanics 12(1), 1–30.

Cai, C., Gao, F., Li, G., Huang, Z., Hou, P., 2015. Evaluation of coal damage and cracking characteristics due to liquid nitrogen cooling on the basis of the energy evolution laws. Journal of Natural Gas Science & Engineering 29, 30-36.

Cai, C., Li, G., Huang, Z., Shen, Z., Tian, S., Wei, J., 2014. Experimental study of the effect of liquid nitrogen cooling on rock pore structure. Journal of Natural Gas Science & Engineering 21, 507-517.

Cai, J., Wei, W., Hu, X., Liu, R., Wang, J., 2017. Fractal characterization of dynamic fracture network extension in porous media. Fractals 25(02), 1750023.

Caulk, R.A., Ghazanfari, E., Perdrial, J.N., Perdrial, N., 2016. Experimental investigation of fracture aperture and permeability change within Enhanced Geothermal Systems. Geothermics 62, 12-21.

Cha, M., Alqahtani, N.B., Yao, B., Yin, X., Kneafsey, T.J., Wang, L., Wu, Y.S., Miskimins, J.L., 2018. Cryogenic Fracturing of Wellbores Under True Triaxial-Confining Stresses: Experimental Investigation. Spe Journal.

Cha, M., Yin, X., Kneafsey, T., Johanson, B., Alqahtani, N., Miskimins, J., Patterson, T., Wu, Y.S., 2014. Cryogenic fracturing for reservoir stimulation – Laboratory studies. Journal of Petroleum Science & Engineering 124, 436-450.

Charlez, P., Lemonnier, P., Ruffet, C., Bouteca, M.J., Tan, C., 1996. Thermally Induced Fracturing: Analysis of a Field Case in North Sea, European Petroleum Conference.

Enayatpour, S., Oort, E.V., Patzek, T., 2013. FreezeFrac Improves the Productivity of Gas Shales.

Gale, J.F.W., Reed, R.M., Holder, J., 2007. Natural fractures in the Barnett Shale and their importance for hydraulic fracture treatments. Aapg Bulletin 91(4), 603-622.

Grant, M.A., 2015. Physical performance indicators for HDR/EGS projects. Geothermics 63, 2-4.

Grundmann, S., Rodvelt, G., Dials, G., Allen, R., 1998. Cryogenic Nitrogen as a Hydraulic Fracturing Fluid in the Devonian Shale, SPE Eastern Regional Meeting.

Gupta, D.V.S., Bobier, D.M., 1998. The history and success of liquid CO2 and CO2/N2 fracturing system. SPE 40016, 15-18.

Kendrick, D.E., Puskar, M.P., Schlotterbeck, S.T., Ultralightweight proppants: a field study in the Big Sandy field of eastern Kentucky. Society of Petroleum Engineers.

Kim, M., Kemeny, J., 2009. Effect of Thermal Shock And Rapid Unloading On Mechanical Rock Properties. Rock Mechanics & Rock Engineering 47(6), 2005-2019.

Legarth, B., Huenges, E., Zimmermann, G., 2005. Hydraulic fracturing in a sedimentary geothermal reservoir: Results and implications. International Journal of Rock Mechanics and Mining Sciences 42(7-8), 1028-1041.

Li, G., Huang, Z., Tian, S., Shen, Z., 2010. Research and application of water jet technology in well completion and stimulation in China. Petroleum Science 7(2), 239-244.

Liu, R., Yu, L., Jiang, Y., 2016. Fractal analysis of directional permeability of gas shale fracture networks: A numerical study. Journal of Natural Gas Science & Engineering 33, 1330-1341.

McDaniel, B.W., Grundmann, S., Kendrick, W., Wilson, D., Jordan, S., 1997. Field Applications of Cryogenic Nitrogen as a Hydraulic Fracturing Fluid. Jpt Journal of Petroleum Technology 50(3), 38-39.

Nami, P., Schellschmidt, R., Schindler, M., Tischner, T., 2008. Chemical stimulation operations for reservoir development of the deep crystalline HDR/EGS system at Soultz-sous-Forêts (France).

Panel, M.L., 2006. The Future of Geothermal Energy. Impact of Enhanced Geothermal Systems [EGS] on the United States in the 21st century. Geothermics 17(5-6), 881–882.

Perkins, T.K., Gonzalez, J.A., 1985. The Effect of Thermoelastic Stresses on Injection Well Fracturing. Society of Petroleum Engineers Journal 25(1), 78-88.

Roy, A., Perfect, E., Dunne, W.M., McKay, L.D., 2007. Fractal characterization of fracture networks: An improved box-counting technique. Journal of Geophysical Research: Solid Earth 112(B12).

Rudenko, N.S., Schubnikow, L.W., 1968. The viscosity of liquid nitrogen, carbon monoxide, argon and oxygen as a function of temperature. NASA Tech. Transl.

Sheng, M., Li, G., Huang, Z., Tian, S., Qu, H., 2013. Experimental study on hydraulic isolation mechanism during hydra-jet fracturing. Experimental Thermal & Fluid Science 44(1), 722-726.

Shi, Y., Song, X., Li, G., Li, R., Zhang, Y., Wang, G., Zheng, R., Lyu, Z., 2018. Numerical Investigation on Heat Extraction Performance of a Downhole Heat Exchanger Geothermal System. Applied Thermal Engineering.

Sun, F., Yao, Y., Chen, M., Li, X., Zhao, L., Meng, Y., Sun, Z., Zhang, T., Feng, D., 2017. Performance analysis of superheated steam injection for heavy oil recovery and modeling of wellbore heat efficiency. Energy 125.

Wang, G., Li, K., Wen, D., Lin, W., Lin, L., Liu, Z., Zhang, W., Ma, F., Wang, W., Assessment of geothermal resources in China. pp. 11-13.

Wang, W., Shahvali, M., Su, Y., 2015. A semi-analytical fractal model for production from tight oil reservoirs with hydraulically fractured horizontal wells. Fuel 158, 612-618.

Xu, P., Cuihong, L.I., Qiu, S., Sasmito, A.P., 2016. A FRACTAL NETWORK MODEL FOR FRACTURED POROUS MEDIA. Fractals-complex Geometry Patterns & Scaling in Nature & Society 24(02), 1650018.

Zhang, S., Huang, Z., Huang, P., Wu, X., Xiong, C., Zhang, C., 2017. Numerical and experimental analysis of hot dry rock fracturing stimulation with high-pressure abrasive liquid nitrogen jet. Journal of Petroleum Science and Engineering.

Zhang, S., Huang, Z., Huang, P., Wu, X., Xiong, C., Zhang, C., 2018a. Numerical and experimental analysis of hot dry rock fracturing stimulation with high-pressure abrasive liquid nitrogen jet. Journal of Petroleum Science and Engineering 163, 156-165.

Zhang, S., Huang, Z., Li, G., Wu, X., Peng, C., Zhang, W., 2018b. Numerical analysis of transient conjugate heat transfer and thermal stress distribution in geothermal drilling with high-pressure liquid nitrogen jet. Applied Thermal Engineering 129, 1348-1357.

Zhang, X., Sanderson, D.J., 1994. Fractal structure and deformation of fractured rock masses, Fractals and Dynamic Systems in Geoscience. Springer, pp. 37-52.

Zhou, C., Wan, Z., Zhang, Y., Gu, B., 2018. Experimental study on hydraulic fracturing of granite under thermal shock. Geothermics 71, 146-155.

Zimmermann, G., Reinicke, A., 2010. Hydraulic stimulation of a deep sandstone reservoir to develop an Enhanced Geothermal System: Laboratory and field experiments. Geothermics 39(1), 70-77.